

REGISTRATION OF AIRBORNE LASER DATA WITH ONE AERIAL IMAGE

Michel ROUX

GET - Télécom-Paris - UMR 5141 LTCI - Département TSI
46 rue Barrault, 75013 Paris - France
michel.roux@enst.fr

KEY WORDS: Airborne Laser Scanner Data, Aerial Image, Image Segmentation, Registration

ABSTRACT

At present, the calibration of airborne laser scanner data relies on the estimation of the position and attitude of the aircraft during the acquisition using GPS and INS systems, but also on the estimation of some other parameters: time bias, scan angle offset, etc, which usually requires the acquisition of extra data over known features: along and across the airport runway, over an horizontal building edge, etc. The operator need then to identify within the cloud of 3D points the position of these known features.

The aim of this paper is to propose a tool for the automated registration of airborne laser scanner data with one aerial image over urban areas. The method makes use of the intrinsic rigidity of the aerial image: the registration is performed by optimizing the 3D reconstruction of the scene calculated with the aerial image and the laser points. On the assumption that urban areas are mainly composed of planar surfaces, a segmentation algorithm generates a partition of the aerial image and a robust technique estimates a 3D plane for each region. The quality of the registration is calculated according to the global number of outliers remaining after the robust estimation.

Experimental results show the convexity of this registration estimator for some low frequency deformations: 3D translations and rotations, and also curvature along and across the flying direction. The system then uses a Nelder-Mead simplex algorithm to calculate a precise registration of both data sets.

1 INTRODUCTION

The calibration of airborne laser acquisition systems is a complex task: its goal is first to identify the systematic errors and then to correct the raw laser data. The different components (the scanner, the GPS and INS systems, etc.) should be calibrated separately, as well as the complete mounted system. Part of the calibration is performed on the ground, but several parameters require also in flight calibration, which supposes the acquisition of extra data over perfectly known features before and after, even during, the acquisition of the data of interest for the mission. The detection and the estimation of systematic errors from these extra data is usually carried out interactively, which reduces the automation of the complete process and causes delays in the delivery of the final data.

Different studies have been dedicated to the modeling of systematic errors in laser acquisition systems (Baltasvias, 1999, Schenk, 2001). Among the identified sources of error, two classes appear: sources of global deformation of the 3D points cloud, and sources of local perturbations. For instance, range error generates a local translation, whose magnitude is constant, but its direction depends of the relative position of the point and the scanner. On the other hand, the mis-alignment of the laser system with the vertical direction generates a global rotation of the 3D points.

The goal of the present paper is to propose an automatic tool to help for the recovery of systematic errors leading to a global deformation of the 3D points. The method is based on the automatic registration of the laser data with a pre-calibrated aerial image. The method is based on the estimation of the quality of the 3D surface reconstruction using both data sets.

A previous study was dealing with the registration of laser data with a digital elevation model generated from aerial images with a classical stereo-restitution approach (Bretar et al., 2003). The new method presented here has the advantage to require only one

image, and to avoid the calculation of a 3D reconstruction from aerial images which may be the source of additional errors.

The next section presents the image segmentation tool and the different approaches tested for the estimation of a planar surface for each region. The section 3 proposes a quality criterion for the evaluation of a 3D reconstruction calculated with both data. The convexity of this criterion for different relative deformations shows its adequation for the automatic registration of one aerial image with the 3D points acquired by a laser scanner system. The section 4 presents briefly the approach developed for the automated registration which is based on a simplex method, and gives the results of the registration for a scene in the suburb of Brussels.

2 3D SURFACE ESTIMATION

We first briefly describe the algorithm used for the segmentation of the aerial image into regions, and then we investigate several techniques for the estimation of a plane from a set of 3D points.

2.1 Image segmentation

The partitioning of the image into meaningful regions is of great interest for aerial images of urban areas since it may provide a useful detection of main components: buildings, roads, cars, etc., which will have individual properties in term of geometry and therefore of models. Region-based segmentation of aerial images is justified because of the specific properties of urban areas: man-made structures often have rather constant albedo as they are often built with a single material.

Split-and-merge techniques for region-based segmentation have shown their ability to generate consistent and robust partitions. Among them, the algorithm proposed by Suk and Chung has the advantage to be a fast and performing technique (Suk and Chung, 1983). This operator is controlled with 3 parameters: each of the

split and merge predicates uses one parameter, the last parameter gives the minimum surface of a region in the final segmentation. The adaptation of this algorithm to colour images in RGB or $L^*a^*b^*$ spaces, and an evaluation of segmentation strategies are presented in (Roux et al., 1997).

The figure 1 shows the result of the region-based segmentation over a small part of an aerial image.

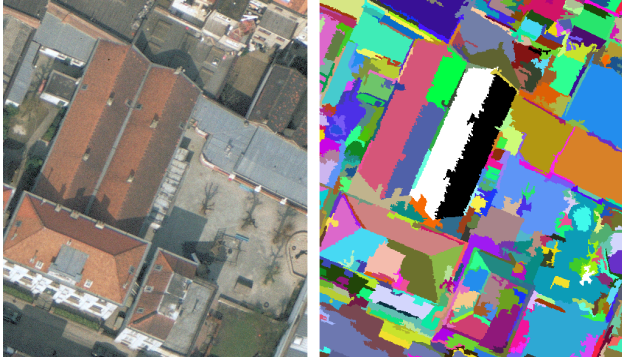


Figure 1: Part of the original image (©EUROSENSE) and result of the segmentation.

2.2 Planar estimation

We propose to investigate different approaches for the estimation of a 3D plane for each region of the segmentation. The plane is estimated with all the laser points whose projection using the collinearity equation falls inside the region (see figure 2).

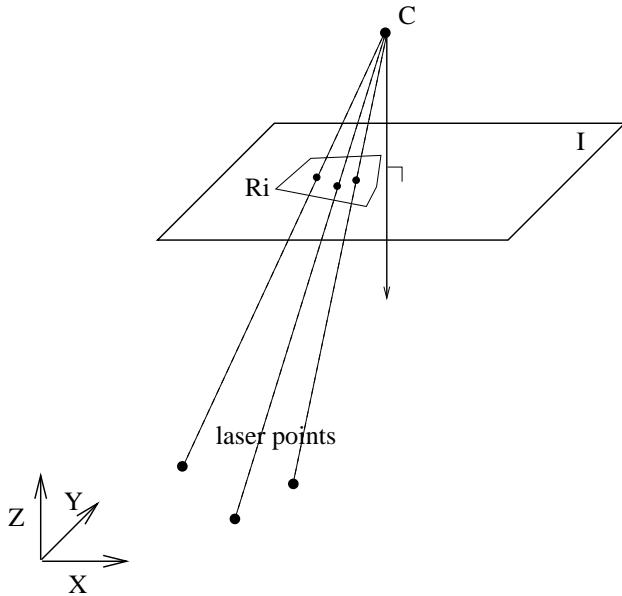


Figure 2: Projection of the laser points in the image plane, and attribution to the regions of the segmentation.

Given N laser points $(x_i, y_i, z_i)_{i=1..N}$, the problem is to estimate the equation of a plane as:

$$a \times x + b \times y + c \times z + d = 0$$

or, if vertical and near-vertical faces are disregarded:

$$z = a \times x + b \times y + c$$

Two types of parameter estimation techniques can be evocated: linear and non-linear approaches. Among the first ones, the least

squares estimator has been widely adopted because its ease of computation. On the other hand, non-linear techniques proved to be robust to the presence of outliers: the LMedS and the RANSAC estimators have also been tested for this application. An extensive tutorial on parameter estimation can be found in (Zhang, 1997).

Least Squares Estimation (LSE): in the case of the second plane equation, the LSE approach consists in the minimization of the mean quadratic error:

$$e = \sqrt{\frac{\sum_{i=1..N} (a \times x_i + b \times y_i + c - z_i)^2}{N}}$$

The solution is given by:

$$\begin{pmatrix} a \\ b \\ c \end{pmatrix} = \begin{pmatrix} \sum x_i^2 & \sum x_i y_i & \sum x_i \\ \sum x_i y_i & \sum y_i^2 & \sum y_i \\ \sum x_i & \sum y_i & N \end{pmatrix}^{-1} \begin{pmatrix} \sum x_i z_i \\ \sum y_i z_i \\ \sum z_i \end{pmatrix}$$

The figure 3 presents 2 views of the 3D reconstruction for the black and white regions of the figure 1. These examples show clearly the inadequacy of the LSE approach when outliers are present in the set of 3D points. One way to overcome this behaviour would be to replace the LSE, i.e. minimization of $\sum_i e_i^2$, with one M-estimator, i.e. minimization of $\sum_i \rho(e_i^2)$, where ρ is positive and symmetric function with a unique minimum at zero (Rousseeuw and Leroy, 1987).

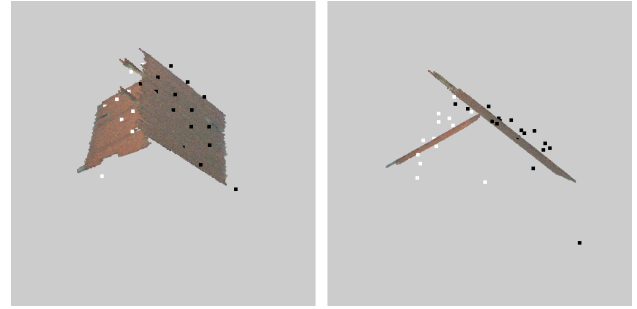


Figure 3: Two views of the 3D reconstruction of 2 regions using the LSE approach.

Least Median of Squares (LMedS): the LMedS estimates the parameters of a shape by solving the non-linear minimization problem:

$$\min \text{median}_i r_i^2$$

where r_i is the residual at the point i . This problem does not have an analytical solution. It is solved with a search in a large set of possible models generated with the data:

- select n features randomly, and estimate the corresponding model,
- calculate the residual to the model for each feature,
- sort the square residuals and select the median value as quality measure for the estimated model,
- repeat previous steps t times and select the model with the better quality measure.

where n is the minimum number of features to calculate a model. In the case of 3D planar surface $n = 3$. The number of iteration t should be large enough to have selected at least one set of n features without outliers. The probability of success or failure can be calculated according to the maximal proportion of outliers α :

$$P_{failure} = (1 - (1 - \alpha)^n)^t$$

In the case of the LMedS estimator $\alpha = 0.5$, but other values may be used according to a priori knowledge on the outlier proportion. The table 1 gives the number of iterations for different values of the probability of failure. The complexity of the LMedS is relatively high: $\mathcal{O}(N \log(N))$, since the residuals of all the features should be sorted.

$P_{failure}$	10^{-1}	10^{-2}	10^{-3}	10^{-4}	10^{-5}
t_{min}	18	35	52	70	87

Table 1: Minimum number of iterations for an expected probability of failure.

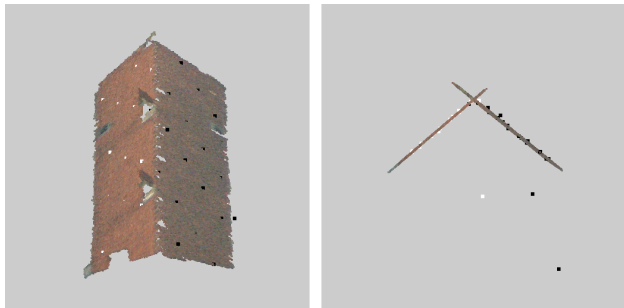


Figure 4: Two views of the 3D reconstruction of 2 regions using the LMedS approach.

The RANSAC algorithm: the Random Sample Consensus has been proposed for the robust estimation of shape parameters (Fischler and Bolles, 1981). It is very similar to the LMedS. As principal difference, the RANSAC requires the operator to give a tolerance threshold to reject a point as outlier for a given model. The outline of the algorithm is the following:

- select n features randomly, and estimate the corresponding model,
- count the number of features which are out a given tolerance ϵ to the model,
- repeat previous steps t times and select the model with the minimum number of outliers.

The RANSAC paradigm can be considered as the dual approach to the LMedS estimation: the RANSAC algorithm optimizes the proportion of features which are within a given error to the model, while the LMedS optimizes the error for a given proportion of features. Both have the same probability of failure. The figures 4 and 5 indicate a similar robustness against outliers for the estimation of planar surfaces. The advantage of the RANSAC over the LMedS is its complexity, which is linear with the total number of features.

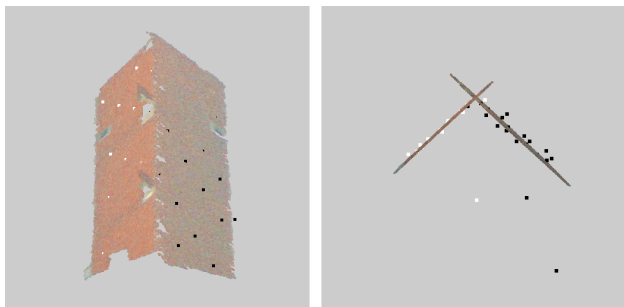


Figure 5: Two views of the 3D reconstruction of 2 regions using the RANSAC approach.

Choice of the estimator: among the three approaches presented above, we retained the RANSAC algorithm, since it has the advantage to be robust to the presence of outliers in the data and to have a complexity which is linear with the number of observations.

The presence of outliers in the data requires some explanation. In the context of 3D plane estimation, the outliers in the image regions have three principal origins:

- some laser points correspond to small structures which are discarded in the segmentation because of the minimum size of the regions: chimneys on the roofs, cars on the streets, etc.,
- the segmentation is far to be perfect and presents over and under-segmentation problems, which are clearly visible on the figure 1,
- a bad localization of the laser point cloud compared to the aerial image generates mis-matches between the laser points and the segmented regions.

The two first sources of outliers correspond to local artifacts in the laser data or in the image segmentation. They are supposed to have negligible effects compared to the third origin of outliers.

3 REGISTRATION AND 3D RECONSTRUCTION

3.1 Evaluation Function

The quality of the 3D reconstruction being used to determine the relative position of the laser points and the optical image, an evaluation function for the 3D reconstruction is needed, whose optimum corresponds to the true relative position. Obviously, the evaluation function should be directly related to the technique involved in the 3D reconstruction. Since we made the choice of the RANSAC approach, the global proportion of outliers calculated with all reconstructed surfaces will serve for the evaluation.

Let $\mathcal{R}_I = \{r_i, i = 1 \dots M\}$ be the partition of the aerial image provided by the segmentation algorithm, \mathcal{L} the set of 3D laser points and f the deformation to be evaluated. We will abusively use the notation $I(p)$ for the projection of a 3D point p in the image plane I using the collinearity equations. Then the set of laser points whose projection in the image after the deformation f falls in a region r_i of the segmentation is noted:

$$\mathcal{L}_{f,r_i} = \{p \in \mathcal{L} / I(f(p)) \in r_i\}$$

The plane estimated with the RANSAC procedure using the 3D points in \mathcal{L}_{f,r_i} is called P_{f,r_i} .

The criterion for the evaluation of the deformation f can then be written as:

$$\varepsilon(f) = \frac{\sum_{r_i \in \mathcal{R}_I} \text{card} \{p \in \mathcal{L}_{f,r_i} / \text{dist}(f(p), P_{f,r_i}) > \epsilon\}}{\sum_{r_i \in \mathcal{R}_I} \text{card} \{\mathcal{L}_{f,r_i}\}}$$

where $\text{dist}(p, P)$ is the Euclidian distance between the point p and the plane P , and ϵ is the tolerance error used in the RANSAC procedure for the estimation of the planes.

3.2 Parametrization of the RANSAC algorithm

Two parameters are involved in the RANSAC algorithm: the number of iterations t and the tolerance ϵ for the detection of the outliers. Experiments have been carried out in order to determine the influence of these parameters.

The figure 6 indicates that a too small value of t generates additional local minima. On the other hand, values larger than 50 do not improve significantly the global convexity of the function.

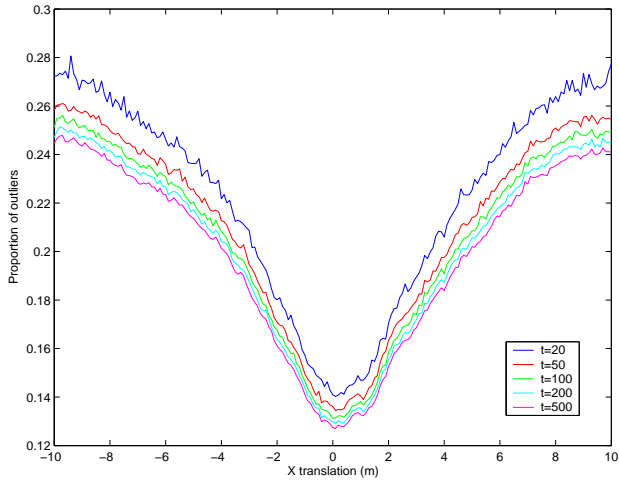


Figure 6: Evaluation function for a translation with different numbers of iterations t in the RANSAC procedure.

The figure 7 shows that a smaller value of ϵ gives a more convex curve, but discards a larger amount of laser points.

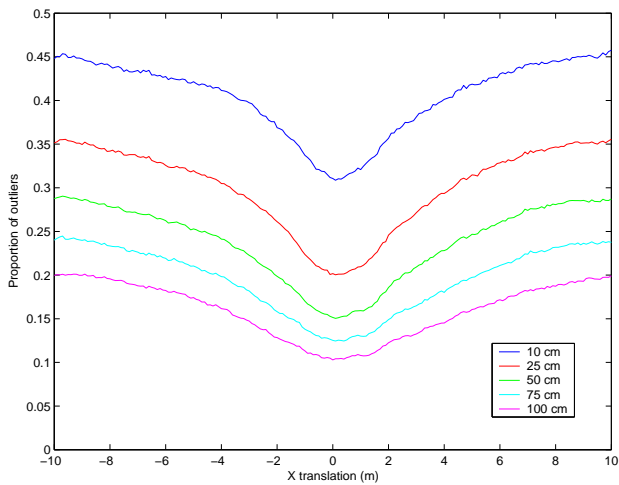


Figure 7: Evaluation function for a translation with different values of the tolerance ϵ in the RANSAC procedure.

For the further experiments presented in this article, the values $t = 50$ and $\epsilon = 50 \text{ cm}$ have been selected. Nevertheless we should point out that the tests were limited to one set of data, and that the stability of the procedure should be evaluated against a larger range of input data characteristics: aerial image resolution, 3D points density, laser accuracy, ...

3.3 Models of deformation

The registration approach has been tested against different deformations applied to a cloud of laser points, which was originally "perfectly" registered with the aerial image. These are mostly rigid deformation: translation and rotation, but also curvature along one of the planimetric directions. The convexity of the evaluation function is tested for each of these deformations.

Planimetric Translation: the figure 8 presents a very sharp global minimum, which may be reached from distances larger than 10 m. This is more than sufficient for an automatic calibration.

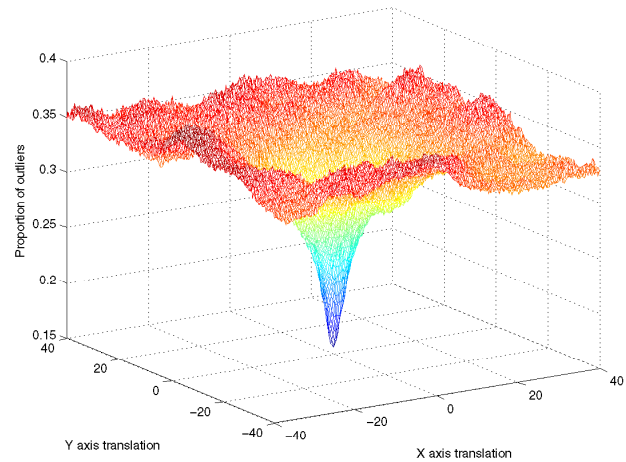


Figure 8: Evaluation function for planimetric translations.

Vertical Translation: on the other hand, the figure 9 indicates that a vertical translation produces also a global minimum, but less sharp than for planimetric translations. We should expect in that case a not so good precision in the registration of the data.

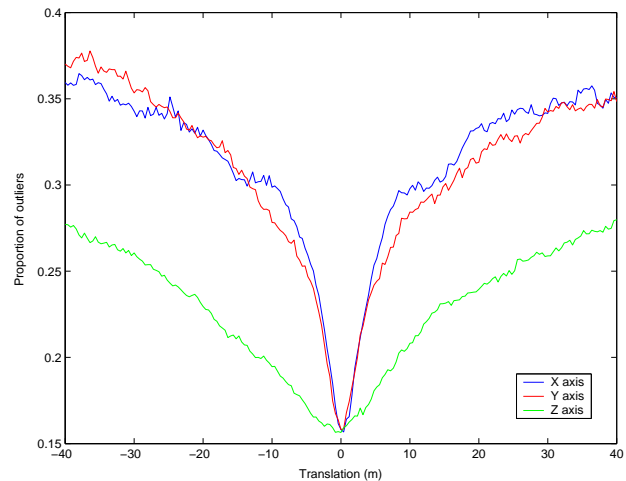


Figure 9: Evaluation function for vertical translations.

Rotation: rotations around the planimetric and the vertical axes present also a different behaviour (see the figure 10). But in that case, the rotations around the vertical axis generate the sharper minimum, which is not of great interest for calibration purposes, since they are less likely to occur than rotations around horizontal axes.

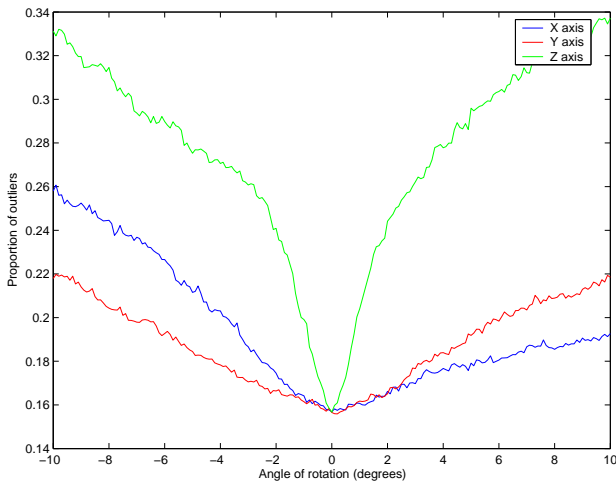


Figure 10: Evaluation function for rotations.

Curvature: the last deformation which have been investigated in this preliminary study is a curvature of the laser points along one of the planimetric direction, as illustrated with the figure 11. This deformation is controlled with a parameter δ , which is related to the curvature radius R via the formula:

$$R = \frac{1 + \delta^2}{2\delta}$$

For $\delta = 0$, the curvature radius is equal to the infinity, i.e. no distortion is applied to the laser points. The parameter δ can take positive and negative values. The two sharp minima on the figure 12 indicate that this kind of deformation could also be estimated with this registration approach.

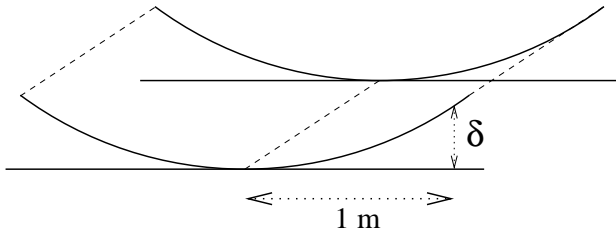


Figure 11: Parametrization of the curvature deformation: δ is the vertical distortion at 1 meter from the curvature axis.

4 AUTOMATIC REGISTRATION

The convexity of the quality criterion demonstrated in the previous section led us to use a simple approach for the automation of the registration. The Nelder-Mead simplex method has the advantage to be very fast to implement and does not require the calculation of the gradient of the evaluation function (Nelder and Mead, 1965).

Presently, the automatic registration procedure is limited to the search of the best planimetric translation, but it can easily be extant to more complex deformations. The data used for this experimentation are presented on the figures 13 and 14. The scene is in the suburb of Brussels and covers a surface of $270 \times 340 m^2$. The aerial image is in colour and has a resolution of 8 cm on the ground. The laser points have been acquired with a oscillating mirror system with a density of $0.32 pt/m^2$. Since both

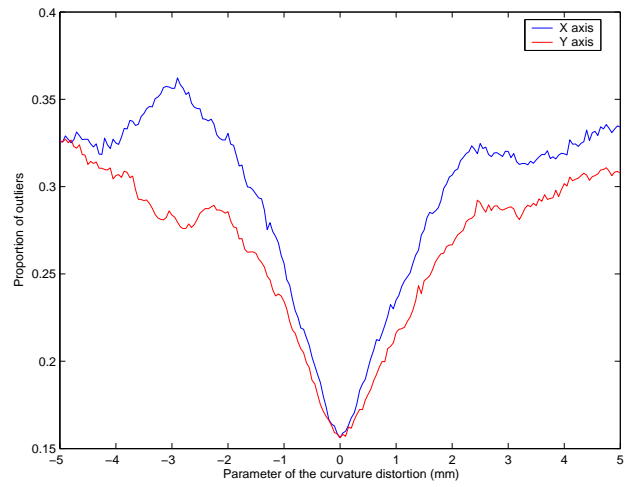


Figure 12: Evaluation function for curvature around X and Y axes.

data were already calibrated, we used the original position as the ground truth.

To test the robustness of the approach, the simplex algorithm was run from 8 initial positions in different directions at a distance larger than 10 meters from the real position. The final positions where close to the ground truth (see table 2), but we noticed a relative dispersion of these local minima.

	original simplex		iterated simplex	
(cm)	X	Y	X	Y
mean	13	0	6	7
std	18	15	2	7
[min , max]	[-8 , 52]	[-35 , 12]	[3 , 9]	[-1 , 15]

Table 2: Statistics for 8 different starting positions with the original and the iterated simplex methods.

In order to improve the stability of the registration process, two solutions may be proposed at the expense of a higher cost in computation time:

- since the simplex shrinks when approaching the minimum of the evaluation function, it may be too small for the last iterations: a solution is to re-run the algorithm from the last position with a relatively large simplex,
- close starting positions may result in different local minima: a solution is to run the simplex algorithm from different starting positions and with different initial simplex size.

The table 2 gives the mean position, the standard deviation and the interval of the 8 final positions obtained with the original simplex procedure, and with the twice iterated procedure. We can notice that with the second method all the final position are grouped within a disk of radius 10 cm.

5 CONCLUSION

A 3D model of an urban scene can be reconstructed with airborne laser data and a single aerial image using robust parameter estimation techniques. We proposed to use the quality of the 3D reconstruction to estimate the relative position of both data, and further to automate their relative registration. A possible application is the automatization of the calibration process for the 3D points acquired with an airborne laser scanning system.



Figure 13: Aerial image in the suburb of Brussels (©EUROSENSE). The scene is $270 \times 340 \text{ m}^2$ and the image has ground resolution of 8 cm.

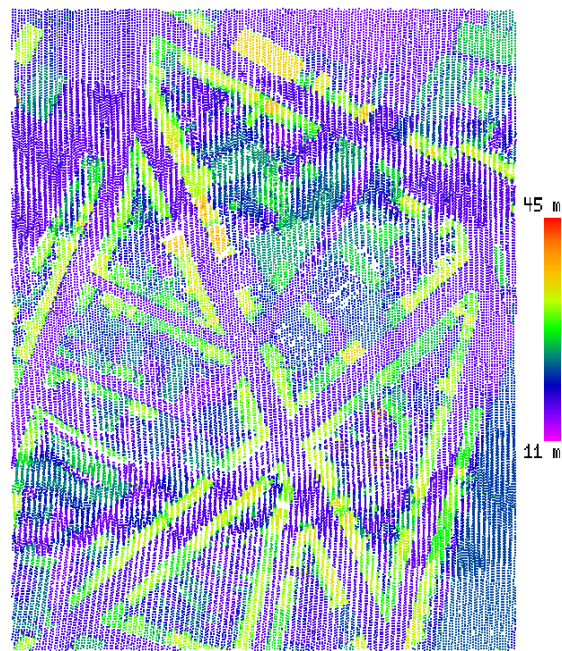


Figure 14: Footprint of the laser points (©EUROSENSE). The elevation is ranging from 11m to 45m.

The 3D reconstruction is performed using robust parameter estimation in order to limit the influence of image segmentation defaults and of the presence of outliers: it is with this aim in view that the RANSAC approach has been selected. The criterion to evaluate the quality of a relative registration of both data is then the proportion of outliers revealed by the RANSAC procedure. Because of the global convexity of this criterion a simple Nelder-Mead simplex method may be used to recover the deformation between the aerial image and the cloud of laser points. The experiments show that rigid deformations can be recovered with this approach.

Further experiments should be undertaken in order to prove the efficiency of the approach for the calibration of airborne laser data:

- application to other data with different characteristics: image resolution, laser scanning systems (oscillating or rotating mirror, optic fibers, ...), laser point density, etc.,
- test for more complex deformations of the laser points cloud: composition of translation, rotation and curvature; and deformations with higher frequencies.
- integration in a global laser point calibration system, especially verify that the precision reachable using this registration approach is sufficient for calibration purposes,

With a different objective than the registration of a laser point cloud and an aerial image, the tools presented in this study may also be of great interest for a fine and detailed 3D reconstruction of a urban scene using 3D laser points and several aerial images.

Acknowledgment: The author is grateful to EUROSENSE for providing the aerial images and the laser points, and to Cyril Minoux for his recursive implementation of the parameter space scanning algorithm.

REFERENCES

- Baltsavias, E., 1999. Airborne laser scanning: basic relations and formulas. *ISPRS Journal of Photogrammetry and Remote Sensing* 54, pp. 199–214.
- Bretar, F., Pierrot-Deseilligny, M. and Roux, M., 2003. Estimating intrinsic accuracy of airborne laser data with local 3d-offsets. In: *Workshop ISPRS on "3-D reconstruction from airborne laser-scanner and InSar data"*, Vol. XXXIV, PART 3/W13, Dresden, Germany.
- Fischler, M. A. and Bolles, R. C., 1981. Random sample consensus: A paradigm for model fitting with applications to image analysis and automated cartography. *Communications of the ACM* 24, pp. 381–395.
- Nelder, J. and Mead, R., 1965. A simplex method for function minimization. *Computer Journal* 7, pp. 308–313.
- Rousseeuw, P. and Leroy, A., 1987. *Robust Regression and Outlier Detection*. John Wiley & Sons, New York.
- Roux, M., Maître, H. and Girard, S., 1997. A step towards stereo reconstruction of urban aerial images. In: *Joint ISPRS Commission III/IV Workshop on 3D Reconstruction and Modelling of Topographic Objects*, Vol. 32, part 3-4W2, Stuttgart (Germany), pp. 107–114.
- Schenk, T., 2001. Modeling and analyzing systematic errors in airborne laser scanners. Technical report, The Ohio State University. *Technical Notes in Photogrammetry* No 19.
- Suk, M. and Chung, S. M., 1983. A new image segmentation technique based on partition mode test. *Pattern Recognition* 16(5), pp. 469–480.
- Zhang, Z., 1997. Parameter estimation technique: a tutorial with application to conic fitting. *Image Vision Computing* 15, pp. 59–76.